PLANT SIGNALING & BEHAVIOR
2023, VOL. 18, NO. 1, e2204654 (12 pages)
https://doi.org/10.1080/15592324.2023.2204654

Taylor & Francis
Taylor & Francis Group

RESEARCH PAPER

OPEN ACCESS Check for updates

# Genome-wide identification of the glutamate receptor-like gene family in *Vanilla planifolia* and their response to *Fusarium oxysporum* infection

Miao Zhu and Xinran Li

School of Biological Science and Technology, Liupanshui Normal University, Liupanshui, Guizhou, China

**ABSTRACT**

Glutamate receptor-like genes (*GLRs*) are essential for plant growth and development and for coping with environmental (biological and non-biological) stresses. In this study, 13 *GLR* members were identified in the *Vanilla planifolia* genome and attributed to two subgroups (Clade I and Clade III) based on their physical relationships. *Cis*-acting element analysis and Gene Ontology (GO) and Kyoto Encyclopedia of Genes and Genomes (KEGG) annotations indicated the GLR gene regulation's complexity and their functional diversity. Expression analysis revealed a relatively higher and more general expression pattern of Clade III members compared to the Clade I subgroup in tissues. Most *GLRs* showed significant differences in expression during *Fusarium oxysporum* infection. This suggested that GLRs play a critical role in the response of *V. planifolia* to pathogenic infection. These results provide helpful information for further functional research and crop improvement of *VpGLRs*.

**ARTICLE HISTORY**
Received 28 January 2023
Revised 20 March 2023
Accepted 21 March 2023

**KEYWORDS**
*Vanilla planifolia*; glutamate receptor-like genes; expression pattern; *Fusarium oxysporum*; biotic stress

## 1. Introduction

Ionotropic glutamate receptor (iGluR) genes are widely studied in mammals. Their encoded proteins function as glutamate-activated ion channels in rapid synaptic transmission and may regulate various neurological, mental, and emotional disorders[1,2]. Unlike mammalian *iGluRs*, glutamate receptor-like genes (*GLRs*) were later discovered in plants. Upon completing the *Arabidopsis thaliana* genome sequencing project, *GLR* was discovered in the plant (*A. thaliana*) in 1998 for the first time[3], which was a homolog of mammalian *iGluR*. There are 20 AtGLR genes in *A. thaliana* and they are subdivided into three clades[4,5]. *GLR* regulates pollen tube growth and morphogenesis in tobacco and *Arabidopsis*[6]. *OsGLR3.4* regulates rice root growth and promotes nitrate absorption by the roots[7]. *AtGLR1.1* and *AtGLR3.7* participate in abscisic acid signal transduction and regulate seed germination[8,9]. *AtGLR1.2* and *AtGLR1.3* are positive regulators of cold resistance and promote jasmonate accumulation to cope with cold stress[10]. Overexpression of *OsGLR1* or *OsGLR2* confers enhanced drought tolerance in *Oryza sativa* and *A. thaliana*[11]. GLR also plays a vital role in plant responses to biotic stress[12]. Triple mutant *GLR2.7*/*GLR2.8*/*GLR2.9 Arabidopsis* exhibited a more susceptible phenotype in response to *Pseudomonas syringae* pv. *tomato* DC3000 infection[13]. *GLR3.3* and *GLR3.5* were involved in the defense response of tomatoes against *Botrytis cinerea* through electrical signaling[14]. According to previous studies, GLRs are essential for plant growth and development, and associated with various physiological and biochemical processes, including disease resistance.

*V. planifolia* is a tropical vine of the Orchidaceae family. It contains a precious natural flavoring renowned for its application in spices[15]. As the only edible spice in the Orchidaceae family[16], it has been widely applied in food, medicine, cosmetics, and other related industries[17,18]. However, its production is severely restricted by pathogenic infections in some producing areas[19]. A common disease is root and stem rot (RSR) caused by *Fusarium oxysporum*; this can drive the necrosis and decay of roots and stems and lead to significant economic losses for *V. planifolia* planting[20,21]. It is unclear if GLR plays a role in *V. planifolia* defense against pathogens.

This study identified *VpGLR* through genome-wide analysis and comprehensive analysis of the characteristics of VpGLR. Meanwhile, the expression pattern of *VpGLRs* in various tissues and after infection by *F. oxysporum* were assessed. This study aimed to provide helpful information to further explore the function of *VpGLR* and offer new options for improving the fungal resistance of *V. planifolia*.

## 2. Materials and methods

### 2.1 Identification and phylogenetic analysis of VpGLRs

Genomic sequences of *V. planifolia*, 20 AtGLRs, and 13 OsGLRs were retrieved from NCBI (https://www.ncbi.nlm.nih.gov/genome/), TAIR (https://www.arabidopsis.org/), and Phytozome (https://phytozome-next.jgi.doe.gov/), respectively. They were used as decoys to retrieve VpGLR family members at the genome-wide level by BLASTP with an e-value cutoff of $1e^{-5}$. The hidden Markov model (HMM) profiles of the GLR domain (PF00060, PF00497, PF01094, PF01609, and PF10613) were acquired from the Pfam database (http://pfam.xfam.

**CONTACT** Xinran Li lixr1219@126.com School of Biological Science and Technology, Liupanshui normal University, No.288 Minghu Road, Liupanshui, Guizhou, China

© 2023 The Author(s). Published with license by Taylor & Francis Group, LLC.
This is an Open Access article distributed under the terms of the Creative Commons Attribution-NonCommercial License (http://creativecommons.org/licenses/by-nc/4.0/), which permits unrestricted non-commercial use, distribution, and reproduction in any medium, provided the original work is properly cited. The terms on which this article has been published allow the posting of the Accepted Manuscript in a repository by the author(s) or with their consent.

org/). They were used to search for possible VpGLR family members of *V. planifolia* using HMMER v3.0, with an e-value cutoff of $1e^{-5}$. The two queries were merged, followed by verification of the VpGLR genes using SMART (http://smart.embl-heidelberg.de/) with an e-value $<1 \times 10^{-5}$.

All GLR proteins from *A. thaliana*, *O. sativa*, and *V. planifolia* were aligned using MAFFT[22], and a maximum likelihood tree (ML tree) was constructed with 1000 guided replications using IQtree (v2.2)[23]. The result was visualized by MEGA X[24].

### 2.2 Molecular characteristics, chromosomal localization, and selection pressure analysis

ExPASY (https://www.expasy.org/) was used to analyze the amino acid number, molecular weight (MW), isoelectric point (pI), instability index, aliphatic index, and grand average hydropathicity (GRAVY)[25]. WoLF PSORT (https://wolfpsort.hgc.jp/) was used to predict the subcellular localization of the proteins[26]. TMHMM-2.0 (https://services.healthtech.dtu.dk/services/TMHMM-2.0/) was used to determine the presence of transmembrane helices (TMHs) in proteins[27]. MG2C (http://mg2c.iask.in/mg2c_v2.1/) was used to analyze the chromosomal location of VpGLR genes[28]. Multiplex linear scanning (MCScan X) was used to detect segmental and tandem duplication genes in the *VpGLRs*[29]. The nonsynonymous substitution rate (Ka), synonymous substitution rate (Ks), and Ka/Ks ratio for each pair of duplicated genes were calculated using MEGA X software.

### 2.3 Conserved motif, gene structure, cis-regulatory elements, and function annotation analysis

Ten conserved motifs of VpGLR proteins were analyzed using the MEME tool (https://meme-suite.org/meme/) with default parameters[30]. The exon-intron distributions of VpGLR genes were analyzed using the Gene Structure Display Server 2.0 (GSDS 2.0) (http://gsds.gao-lab.org/) according to the Generic Feature Format Version 3 (GFF3) genome annotation files[31]. Two kb sequences up-stream of the start codon of VpGLR genes were extracted as their promoter sequences, which were identified using the PlantCARE tool (http://bioinformatics.psb.ugent.be/webtools/plantcare/html/)[32]. The key elements were further classified, summarized, and mapped using the GSDS 2.0. Gene Ontology (GO) and KEGG functional annotations of *VpGLRs* was performed using eggnog-MAPPER (http://eggnog-mapper.embl.de/)[33] and visualized by Tbtools[34].

### 2.4 GLR gene expression analysis by RNA-seq data

RNA-Seq data (accession numbers SRP043630 and SRP214274) were obtained from the Sequence Read Archive (SRA) database to investigate the expression patterns of VpGLR genes in different tissues and biotic stress processes after infection with *F. oxysporum*. The details of growth conditions and treatment conditions were as described by Rao et al.[35] and Solano-De et al.[20] respectively. The expression pattern of different tissues was obtained at the age of six months: leaf, stem, mesocarp, placental laminae, hair cells, and seeds. Biotic stress analysis obtained RNA-Seq data after the roots were infected for two days and ten days compared with uninfected plants after 12 weeks of cultivation at room temperature. Trimmomatic, SAMtools, and StringTie were performed for data quality control, creation of the BAM file, and abundance calculation. The GLR expression spectrum was normalized (fragments per kilobase of exon per million reads, FPKM+1) by log2 transformation and then visualization by Tbtools[34]. A change in expression by a factor of ≥ 2 fold indicates significant differences between the groups.

## 3 Results

### 3.1 Protein properties and phylogenetic analysis of VpGLRs

Thirteen VpGLR genes were identified from the genome of *V. planifolia* and named according to their chromosomal location information and phylogenetic relationships (Table 1 and Figure 1). In short, the number of amino acids was between 438 (VpGLR3.2) and 981 (VpGLR1.2), and the molecular weight (MW) was between 48.36 kDa (VpGLR3.2) and 108.50 kDa (VpGLR1.1). VpGLR3.3 and VpGLR1.4 possessed the highest (8.96) and lowest (5.12) isoelectric points, respectively. VpGLR1.7 had the highest number (6) of transmembrane domains, while VpGLR3.1 and VpGLR3.2 had none. Most were predicted to be localized in the plasma membrane except for VpGLR1.6 (endoplasmic reticulum), VpGLR3.1 (chloroplast), and VpGLR3.2 (located in the mitochondria). Five out of thirteen were classified as hydrophilic (grand average of hydropathicity (GRAVY) index<0).

We introduced 20 AtGLRs and 13 OsGLRs to construct the evolutionary relationship of VpGLRs more clearly. All the GLRs participating in building the evolutionary tree were divided into two groups (Figure 1). The VpGLRs clustered with *Arabidopsis* and rice's Clade I members were designated as VpGLR1.1-VpGLR1.7 following previous naming conventions. In contrast, the remaining VpGLRs (VpGLR3.1-VpGLR3.6) clustered with Clade III members. The evolutionary relationship between the VpGLRs and OsGLRs was closer than that of AtGLRs.

### 3.2 Conserved motifs and gene structure of VpGLRs

This motif is closely related to the biological function of the protein, and we scanned the motifs in the 13 VpGLR members. As shown in Figure 2, the results revealed ten motifs in VpGLRs, and detailed information of these motifs was shown in Table 2. Two of the ten identified motifs (motif one and motif 10) contained the Lig_chan domain. This represents the ligand-gated ion channel super-family, including four transmembrane regions (M1, M2, M3, and M4). Motifs 2, 5, 8, and 9 belong to the peripheral binding protein type 2 superfamily that contains ligand-binding domain residues. Motifs 3, 4, and 6 contain the ANF receptor domain belonging to the type 1 periplasmic binding-fold superfamily. VpGLR1.1, VpGLR1.2, VpGLR1.4, and VpGLR3.4 had the most motifs, while VpGLR3.2 contained the least motifs. Motif 10 only existed

**Table 1.** Basic information for the Vanilla planifolia glutamate receptor-like genes VpGLR gene family members.

| Gene name | Gene ID | Chromosome location | Size (aa) | MW (kDa) | pI | TD | SL | Instability index | Aliphatic index | GRAVY |
|---|---|---|---|---|---|---|---|---|---|---|
| *VpGLR1.1* | Vpl05Ag10477 | Chr5:5575246–5584481 | 965 | 108.50 | 5.21 | 4 | plas | 37.78 | 92.99 | −0.038 |
| *VpGLR1.2* | Vpl05Ag10758 | Chr5:9299996–9303584 | 981 | 107.22 | 8.48 | 3 | plas | 41.94 | 88.40 | 0.023 |
| *VpGLR1.3* | Vpl05Ag12402 | Chr5:48784160–48794538 | 776 | 86.28 | 6.98 | 2 | plas | 36.88 | 89.07 | −0.061 |
| *VpGLR1.4* | Vpl08Ag17148 | Chr8:27407012–27410142 | 953 | 104.77 | 5.12 | 3 | plas | 36.35 | 87.04 | 0.049 |
| *VpGLR1.5* | Vpl08Ag17149 | Chr8:27433144–27453280 | 463 | 52.24 | 5.84 | 3 | plas | 35.91 | 93.09 | −0.034 |
| *VpGLR1.6* | Vpl08Ag17155 | Chr8:27700702–27709385 | 869 | 98.08 | 8.59 | 3 | ER | 37.25 | 97.15 | 0.028 |
| *VpGLR1.7* | Vpl08Ag17156 | Chr8:27743951–27747073 | 751 | 82.93 | 5.30 | 6 | plas | 40.33 | 90.61 | 0.082 |
| *VpGLR3.1* | Vpl01Ag03715 | Chr1:67431928–67471016 | 649 | 71.34 | 5.39 | 0 | chlo | 34.69 | 99.24 | −0.033 |
| *VpGLR3.2* | Vpl01Ag03721 | Chr1:67651449–67687932 | 438 | 48.36 | 5.36 | 0 | mito | 35.99 | 97.65 | −0.073 |
| *VpGLR3.3* | Vpl01Ag04134 | Chr1:75866947–75877873 | 906 | 100.90 | 8.96 | 3 | plas | 38.43 | 97.40 | 0.108 |
| *VpGLR3.4* | Vpl02Ag05107 | Chr2:19738624–19745750 | 956 | 106.57 | 5.47 | 4 | plas | 42.74 | 92.02 | 0.042 |
| *VpGLR3.5* | Vpl12Ag22538 | Chr12:16954665–16957860 | 844 | 93.80 | 5.20 | 3 | plas | 43.94 | 95.39 | 0.053 |
| *VpGLR3.6* | Vpl13Ag24036 | Chr13:6771823–6783404 | 792 | 86.74 | 6.70 | 3 | plas | 42.17 | 97.11 | 0.148 |

Note: MW, pI, TD, SL and GRAVY are molecular weight, isoelectric point, transmembrane domain, subcellular localization and grand average of hydropathicity, respectively; plas, ER, chlo, and mito indicate the plasma membrane, endoplasmic reticulum, chloroplast, and mitochondria, respectively.

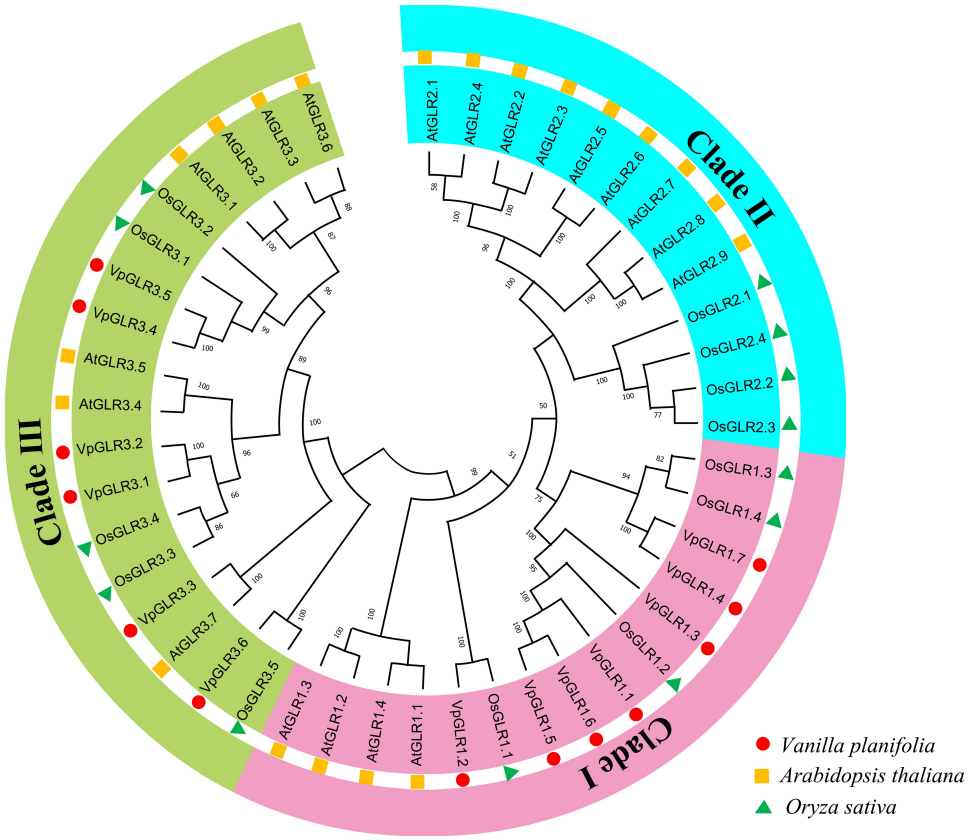


**Figure 1.** Phylogenetic tree of GLR proteins from Arabidopsis, rice, and soybean. All protein sequences were aligned using MAFFT and the maximum likelihood (ML) tree was constructed using IQtree with 1,000 bootstrap replicates. Different colors indicate distinct subgroups or species.

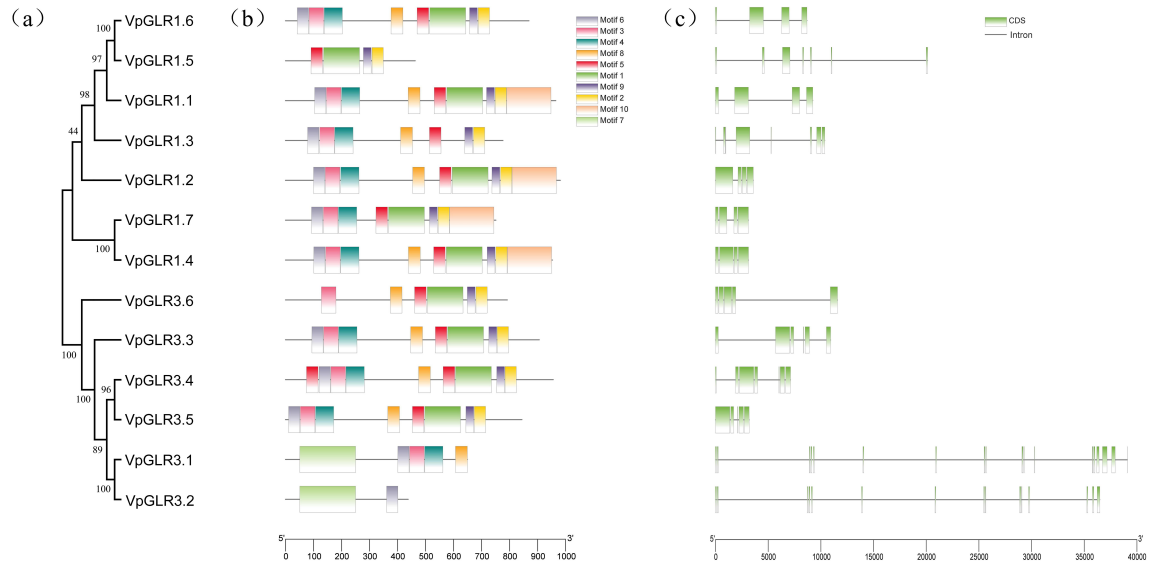


**Figure 2.** Schematic diagram of the phylogenetic tree (a); conserved motif (b); and gene structure (c) of VpGlrs. Genes from the same subtribe were indicated by the same color.

**Table 2.** Multilevel consensus sequences in VpGLP gene family identified by MEME.

| Motifs | Domain | Best possible match | Width(aa) | Sites | *E*-value |
|---|---|---|---|---|---|
| 1 | Lig_chan domain | WIFLKPLTTDLWCVTGAFFIFTGFVVWILEHRINPEFRGPPKDQCGTVFWFSFSTLVFAHREKMLSNLSRFVMIV WVFVVMIIQSSYTASLTSMLTVRQLQPTIRGIDDLIKQGDPVGYQNGSFVPKYL | 129 | 9 | 5.4e-455 |
| 2 | Ligand-binding domain | HCCKYTMVGPIYKTDGWGFAFPRDSPLVPDVSRAILKLTES | 41 | 11 | 1.4e-169 |
| 3 | ANF receptor domain | QYPYFVRTTQSDSYQMKAIAELIQYFGWREVIPIYEDDEYGRGIVPYLIDALQ | 53 | 10 | 3.6e-140 |
| 4 | ANF receptor domain | IDCRIPYKCAIPPQASDDHILEKLYHLKTMQSRVFVVHMTCDLGLRIFHVAHEEGMMTEGYAWIAT | 66 | 9 | 4.4e-135 |
| 5 | Ligand-binding domain | KNFDAVVGDITIMANRSHYVDFTQPYTDSGVSMLVPVKNKEE | 42 | 10 | 1.1e-119 |
| 6 | ANF receptor domain | TDVKAIIGPQTSEEAHFVAELGNEAQVPIISFAATDPSLSS | 41 | 11 | 1.2e-113 |
| 7 | IspD domain | KRMGVSMPKQYLSLLGKPIALYSLFTFSELSEVKEIVVVCEPSYQNLFEDIIEEVNVDIKFAL PGKERQDSVFNGLQEVDGSSELVCIHDSARPLVLSTDVRKVLKDGWLNGAAVLGVPVKATIKEANKD SFVTRTFDRKTLWEMQTPQVIKPDLLRAGFELVNREGLEVTDDASIVEYLSHPVYITEGSYTNIKVTTPD | 200 | 2 | 1.7e-072 |
| 8 | Ligand-binding domain | WPGQTTMVPRGWEWPTNGQKLRIGVPNRPSYPQFVSKEKDPDT | 43 | 7 | 4.5e-070 |
| 9 | Ligand-binding domain | EYPQDYHNGPSNGGVAAIFDEIPYLKIFM | 29 | 10 | 7.4e-069 |
| 10 | Lig_chan domain | DIMMEIERKWFGDQKPCLPQSEGVSSTSLNFSNFGGLFLITGTVSVFALL IYILVFLRKEWDDVRAATLDAGDRGGSFWDKAAALAKHYDSIKEKRGSGTARGN MEQELSCNGIISEGPQTPISISEMSALNCVSQQTVASGRTSTEEMPTEQFIELRG | 159 | 2 | 1.0e-059 |

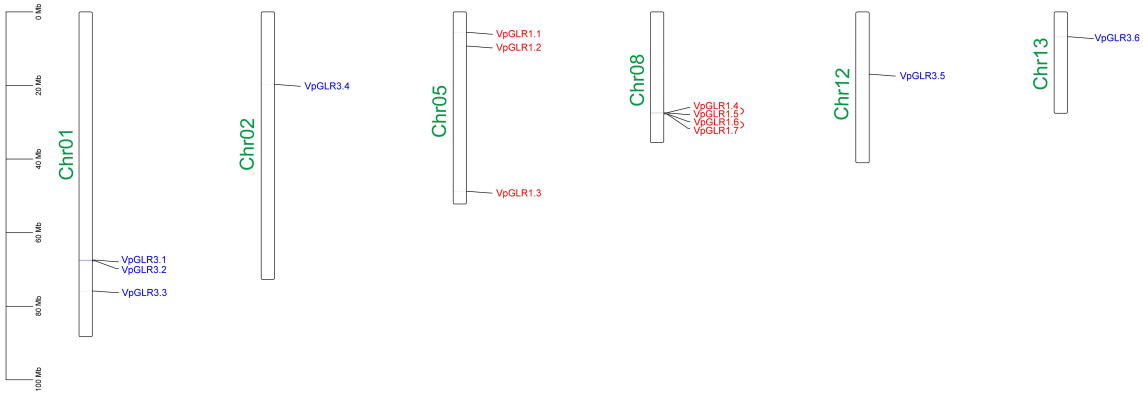


**Figure 3.** Chromosomal distribution of GLR genes in Vanilla planifolia. Chromosome size is indicated by its relative length. Chromosome numbers are shown at the left of each chromosome.

in VpGLR1.1, VpGLR1.2, VpGLR1.4, and VpGLR1.7. Most motifs are widely distributed among VpGLR members. Interestingly, motif 5 appeared twice in VpGLR3.4. *VpGLR3.1* (18) and *VpGLR3.2* (15) possessed more CDSs than the other members. *VpGLR1.1*, *VpGLR1.2*, *VpGLR1.4*, *VpGLR1.6*, and *VpGLR1.7* had the least number (4) of CDSs.

### 3.3 Chromosomal distribution and gene duplication analysis of VpGLR genes

Thirteen VpGLR genes were unequally distributed on six chromosomes of *V. planifolia* (except for *VpGLR3.4* and *VpGLR3.5*), while the other members were distributed close to the chromosome ends (Figure 3). Chr08 possessed the most *VpGLRs* (4) among these six chromosomes, whereas Chr02, Chr12, and Chr13 had only one member.

Two pairs of tandem duplications and one pair of fragment duplication genes were identified in the *VpGLR* family (Table 3). These homologous pairing genes were all members of the Clade I subgroup, and no duplication events were found in Clade III. Interestingly, *VpGLR1.4* was associated with tandem and segmental duplication events. The collinearity of homologous genetic relationships between *VpGLRs*, *OsGLRs*, and *AtGLRs* was analyzed to further understand the GLR gene family amplification mechanism. Three homologous genes were found between *V. planifolia* and *O. sativa* (*VpGLR1.4* and *OsGLR1.1*; *VpGLR1.6* and *OsGLR1.4*; and *VpGLR1.6* and *OsGLR2.2*), and there was no collinearity relationship with *Arabidopsis* (Figure 4). *VpGLR1.4* exhibited collinearity between species, whereas *VpGLR1.6* corresponded to two homologous genes in rice. These results suggested that these genes may have played an essential role in the evolution of the GLR gene family. In addition, the Ka/Ks ratios of all homologous gene pairs were below one.

### 3.4 Cis-acting regulatory elements and analysis

The presence of *cis*-regulatory elements (CAREs) was predicted to further understand the potential transcriptional regulation of *VpGLRs*. Forty-six *cis*-acting regulatory elements were identified. They belonged to five main categories: binding site element (3), stress-induced component (6), growth and development component (5), hormone response (8), and light response element (24) (Figure 5).

Thirty-three Box 4 and thirty-two GT1-motif fragments were present in the promoter region of *VpGLRs*. These two elements were associated with 11 *VpGLRs* each, making them the most widely distributed CAREs. *VpGLR3.5* had the highest number (32) and type (19) of CAREs, whereas *VpGLR1.3* and *VpGLR1.4* contained the least number of CAREs (13), and *VpGLR1.4* also contained the least number of CAREs (10).

### 3.5 Enrichment analysis using GO and KEGG

Gene Ontology (GO) and Kyoto Encyclopedia of Genes and Genomes (KEGG) enrichment analyses were performed to explore the biological function of *VpGLR* at the molecular level. GO annotation for the VpGLR protein was analyzed using molecular function (MF), cellular component (CC), and biological process (BP). Seven of the 13 VpGLR genes were significantly enriched in 60 terms ($p$-value<0.05), including 17 MFs, three CCs, and 40 BPs (Figure 6). The enriched *VpGLR* members were mainly related to ion and protein transport activities in MF ontology. The CC ontology was mainly associated with the components of the cell membrane and the peripheral structure. The BP ontology was mainly involved in regulating cell transport, communication, and reactions.

Further enrichment analysis of KEGG pathways showed that 12 of the 13 members (except for *VpGLR3.2*) were significantly enriched in two pathways: ion channels and protein families (signaling and cellular processes).

### 3.6 Expression patterns of VpGlrs

Gene expression analysis was performed for six different tissues (placenta, hair, seed, leaf, stem, and mesocarp) at the age of six months to understand the expression profiles of the GLR gene family in *V. planifolia*. The expression of different *VpGLR* members considerably varied in the tissues (Figure 7a). Interestingly, *VpGLR* expression in the six tissues occurred in two patterns, except for *VpGLR1.1*. Clade I members had lower overall expression compared with Clade III. Clade I members showed low to moderate expression in hair and seed (except for *VpGLR1.1*, *VpGLR1.4*, and *VpGLR1.7*), and in the leaf, stem,

**Table 3.** Ka/Ks analysis for duplicated GLR genes.

| Gene ID1 | Gene ID2 | Ka | Ks | Ka/Ks | Duplication type |
|---|---|---|---|---|---|
| *VpGLR1.4* | *VpGLR1.5* | 0.5223 | 3.0314 | 0.1723 | Tandem |
| *VpGLR1.6* | *VpGLR1.7* | 0.6233 | 1.4164 | 0.4401 | Tandem |
| *VpGLR1.2* | *VpGLR1.4* | 0.6067 | 0.9883 | 0.6139 | Segmental |
| *VpGLR1.4* | *OsGLR1.1* | 0.6524 | 0.8828 | 0.7390 | Segmental |
| *VpGLR1.6* | *OsGLR1.4* | 0.5181 | 0.8178 | 0.6335 | Segmental |
| *VpGLR1.6* | *OsGLR2.2* | 0.6048 | 1.1692 | 0.5173 | Segmental |

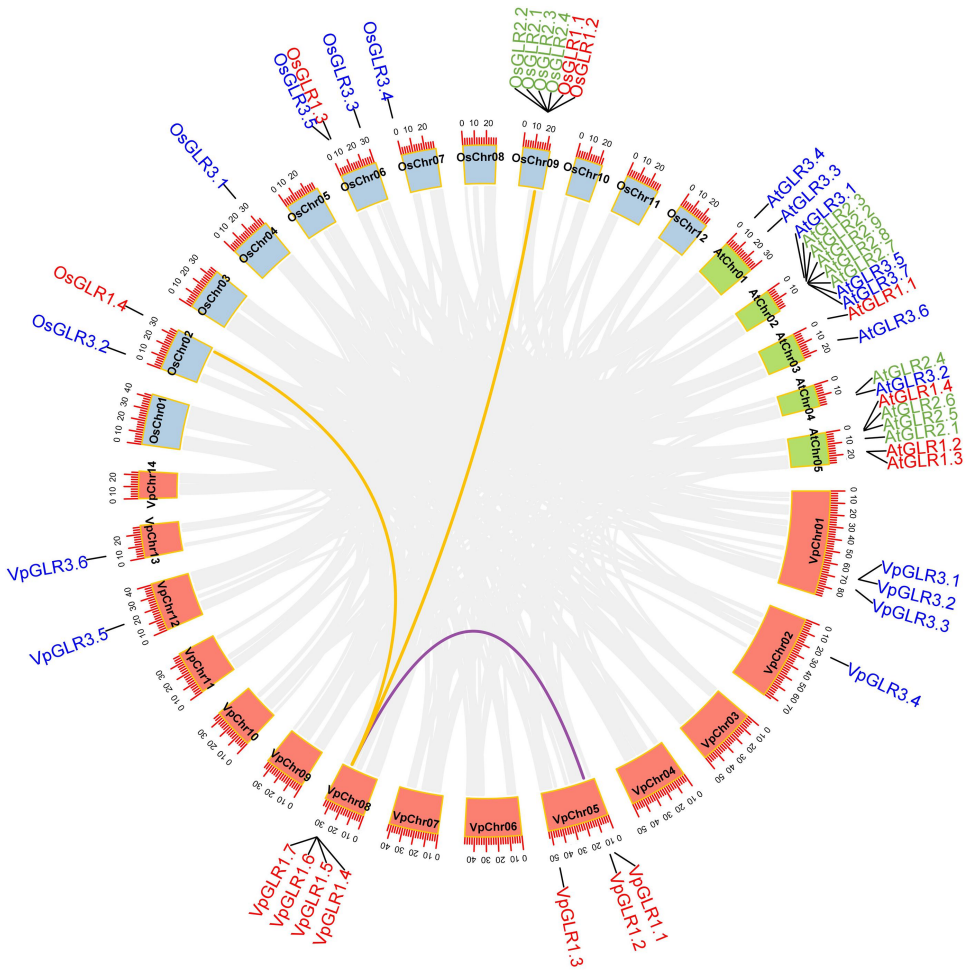


**Figure 4.** Genome-wide synteny analysis of GLRs between Vanilla planifolia, Oryza sativa, and Arabidopsis thaliana. GLRs and chromosomes from the different species were indicated by the different colors.

and mesocarp (except for *VpGLR1.2*). The remaining members had very weak or no expression. All Clade III members were expressed in all six tissues. Among them, *VpGLR3.4* possessed the highest expression in placental, hair, seed, and mesocarp, while *VpGLR3.3* showed the highest expression level in leaves and stems, although this high expression was essentially the same as in *VpGLR3.4*. In addition, *VpGLR1.1* was highly expressed in the mesocarp and *VpGLR3.5* was highly expressed in the placenta, seed, and mesocarp. All the genes involved in high expression may play an essential role in tissue development and metabolism.

Biotic stress was determined by characterizing the expression pattern of the VpGLR gene family using transcriptome data from *F. oxysporum*-infected roots that were cultured at room temperature for 12 weeks before infection. The expression of *VPGLR 1.2*, *VPGLR 1.4*, *VPGLR 1.7*, and *VPGLR 3.3* was significantly increased at two days of infection compared to the uninfected group (Figure 7b). The expression levels of most members (except for *VpGLR1.7* and *VpGLR3.5*) were significantly up-regulated on the 10th day of infection, especially *VpGLR1.1*, *VpGLR1.2*, *VpGLR1.3*, *VpGLR1.6*, and *VpGLR3.2* which increased by at least four-fold.

## 4. Discussion

In recent decades, plant GLRs were proven to play crucial roles in growth and development, signal transduction, and responses to biotic and abiotic stresses[36–38]. However, knowledge of GLRs in *V. planifolia* is limited. In this study, 13 GLRs from *V. planifolia* were identified and clustered into two clades

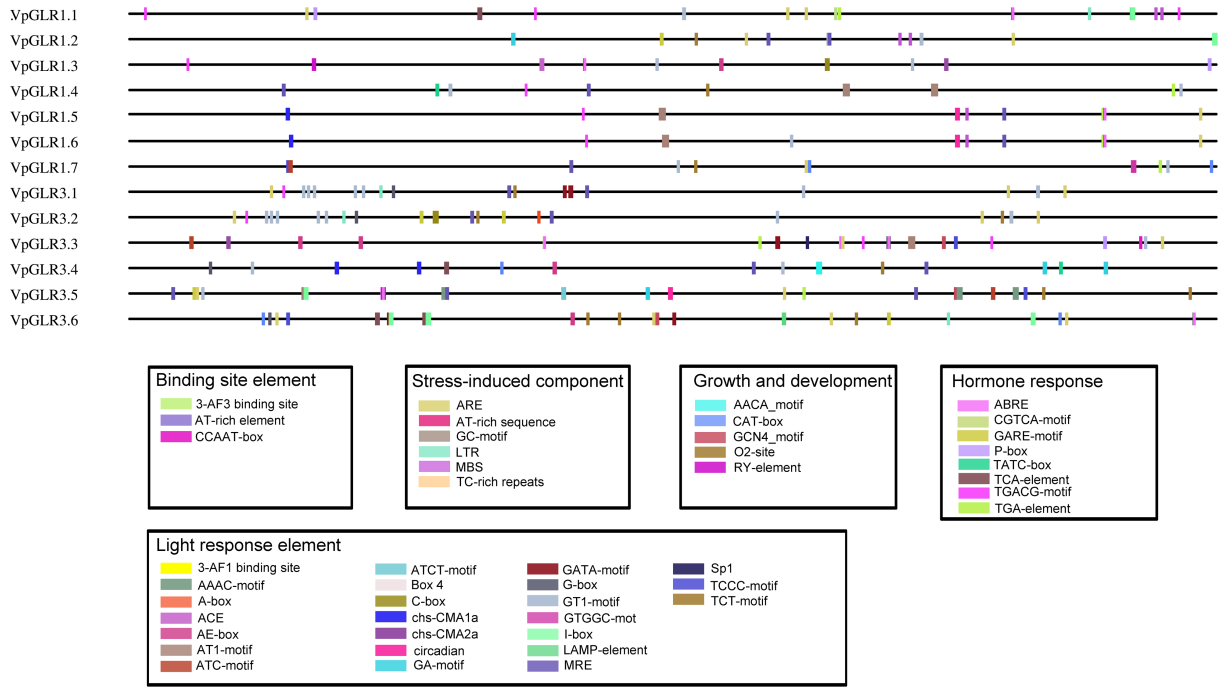


**Figure 5.** The distribution of cis-acting regulatory elements in the promoters of the VpGLR gene family members.

based on phylogenetic relationships. Clade I contained seven members and Clade III contained six members. The GLR gene family is divided into three branches in many plants, including *Arabidopsis*[4], *Solanum lycopersicum*[39], and *Saccharum officinarum*[12]. However, VpGLRs only had two branches and lacked Clade II. *A. thaliana* GLRs in Clade I and Clade II are closely related and belong to sister branches[40]. Clade I and Clade II were attributed to the same large subgroup in the GLR of Rosaceae[41]. Here, the absence of Clade II members was likely due to the fact that Clade I and Clade II members of *V. planifolia* showed closer genetic relationships compared with *O. sativa* GLRs and *A. thaliana* GLRs. In addition, GLR members belonging to these two subgroups were found in *Zea mays*[42] and *Brassica rapa*[43]. These results are consistent with those observed in our phylogenetic tree.

Currently, most GLRs are thought positioned on the cell plasma membrane, with little information available on GLR-targeting organelles and related functions. A splicing variant of AtGLR3.5 is located in the endoplasmic reticulum[44]. Its deletion mutation causes a lightweight reduction of calcium ions in the endoplasmic reticulum, and may affect the shape of the endoplasmic reticulum (ER) and lead to the loss of cristae, while promoting the aging of cells[44]. AtGLR 3.1 and AtGLR3.3 are located in the ER-like structures of xylem contact cells and phloem sieve elements, respectively, and play an essential role in calcium signaling triggered by wounds[45]. Spinach iGLR3 is located in the chloroplast, but its function remains unclear[46]. Mutation of chloroplast localized AtGLR3.4 in *A. thaliana* leads to a slight decrease in photosynthesis[47]. In this study, ten members of 13 VpGLRs were predicted to be located in the plasma membrane. This suggested that most of them play a role in the plasma membrane. VpGLR1.6, VpGLR3.1, and VpGLR3.2 were predicted to be located in the ER, chloroplast, and mitochondria, respectively. Further work is required to determine their actual localization and whether their functions are consistent with the AtGLRs mentioned above.

Gene replication is an essential driver of gene expansion and evolution and plays a significant role in the adaptive evolution of species[48,49]. This study identified two tandem and one segmental duplication among the 13 VpGLR genes. The Ka/Ks ratios of these homologous paired genes were all below 1.0. This indicated that they underwent a purification selection process in evolutionary history to maintain their functions[50]. In addition, collinear analysis of *VpGLRs* among different species showed that *VpGLRs* have no collinear relationship with *GLRs* from the dicotyledonous *Arabidopsis*. However, *VpGLRs* are homologous with *GLRs* from monocotyledonous rice plants. This correlated with a previous study showing that *GLRs* show no collinearity in four dicotyledons and two monocotyledons[12]. Therefore, it is speculated that the generation of homologous GLR genes only occurs after the differentiation of dicotyledonous and monocotyledonous plants.

The expression and distribution of GLR in plant tissues was known as early as the beginning of this century. There are no branch-specific organ expression patterns found for 20 *GLRs* in *A. thaliana*[40]. Similarly, we are yet to find this in *V. planifolia*. However, we found that the expression levels in different tissues were branch-specific, and that the expression levels of Clade III members were generally higher than those of *GLRs* in Clade I. The same situation was observed in sugarcane[12]. This suggests that the *GLRs* of Clade III might have essential roles in plant growth regulation mechanisms. Interestingly, the clustering of Clade I members according to their expression levels in various organizations is surprisingly consistent with the branch they belong to in the evolutionary tree. The aggregation of most Clade I members was entirely consistent with their assemblage in the evolutionary tree except for *VpGLR1.1*,

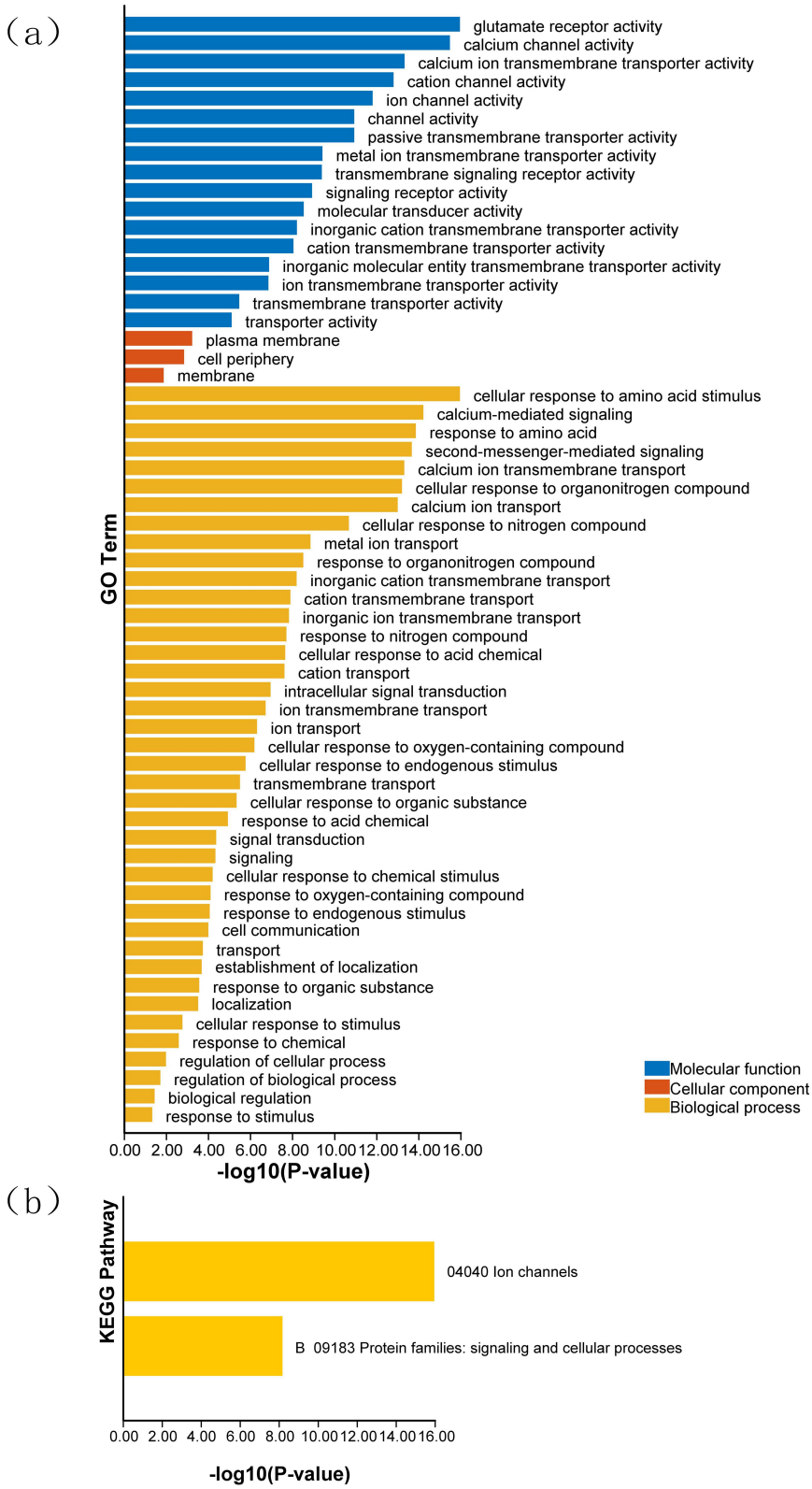


**Figure 6.** Gene Ontology (GO) and Kyoto Encyclopedia of Genes and Genomes (KEGG) enrichment analysis of VpGlrs. (a) Highly enriched GO terms in VpGlrs; (b) highly enriched KEGG pathways in VpGlrs.

which had a relatively high expression and aggregated with Clade III members.

Additionally, GLRs are one of the key molecules in the resistance of plants to pathogenic infections. The use of GLR inhibitors can reduce the host's resistance to pathogenic bacteria. *AtGLR3.3* confers resistance to *Pseudomonas syringae* pv *tomato* DC3000 and *Hyaloperonospora arabidopsidis* in *Arabidopsis*[51,52]. Transgenic *Arabidopsis* seedlings overexpressing small radish *RsGluR* upregulate the expression of jasmonic acid (JA) biosynthesis-related genes and inhibit the growth of

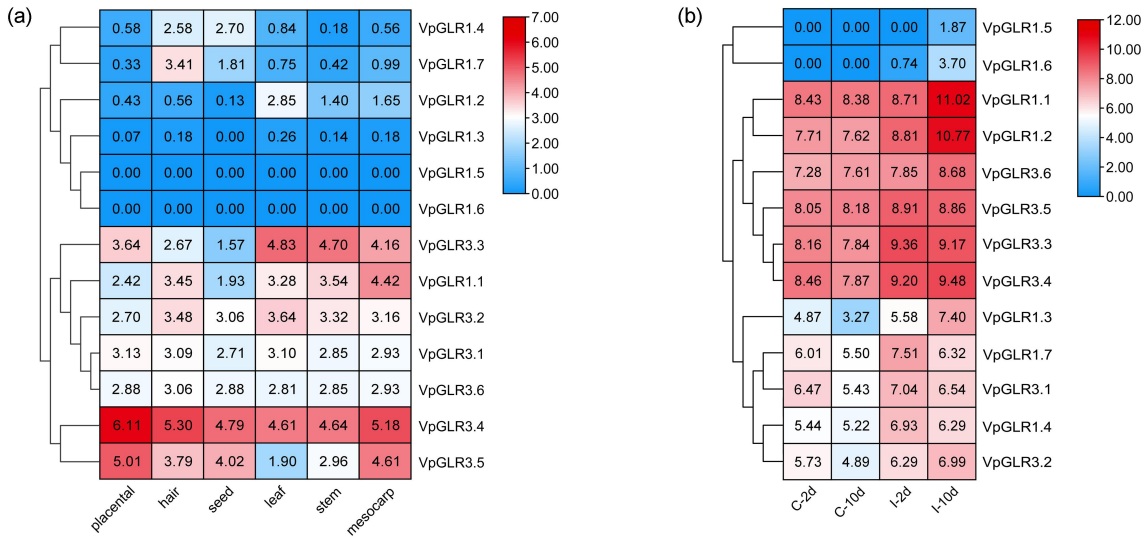


**Figure 7.** Expression profiles of VpGLR genes. (a) Expression pattern of VpGLR genes in different tissues at six months; (b) Expression pattern of VpFAD genes for Fusarium oxysporum-infected roots after 12 weeks of room-temperature culture. "C-2d" denotes untreated by F. oxysporum at two days control group (uninfected group); "C-10d" means untreated by F. oxysporum at ten days control group (uninfected group); "I-2d" represents the infected group at two days after F. oxysporum treatment; "I-10d" indicates the infected group at ten days after F. oxysporum treatment.

the pathogenic fungus, *Botrytis cinerea*[53]. A single nucleotide mutant of *GhGLR4.8* (from *GhGLR4.8C* to *GhGLR4.8A*) confers cotton resistance to *Fusarium oxysporum* f. sp. *Vasinfectum* (fov)[54]. These results suggest that *GLR* overexpression, heterogeneous expression, and genetic engineering modifications can enhance the beneficial immune properties of the host against the pathogen. In contrast, most *VpGLRs* were found to be significantly upregulated during *F. oxysporum* infection in our study, particularly *VpGLR1.1*, *VpGLR1.2*, *VpGLR1.3*, *VpGLR1.6*, and *VpGLR3.2*, which may play an essential role in the infection process, and these genes are potential targets for breeding resistant *V. planifolia*.

## 5. Conclusions

This study identified 13 members of the GLR family in the *V. planifolia* genome and analyzed their basic physicochemical properties, chromosomal distribution, and genetic structural characteristics. They were divided into two large subsets based on phylogenetic relationships: Clades I and III possessed seven and six members, respectively. Prediction of *cis*-acting elements revealed that *VpGLR* expression may be regulated by multiple categories of factors. Gene Ontology and KEGG analyses demonstrated that the molecular functions of *VpGLRs* were diverse. In addition, Clade III members were more commonly expressed in various tissues (and in relatively higher amounts) than Clade I members. Most *GLRs* were significantly upregulated following *F. oxysporum* infection. In particular, *VpGLR1.1*, *VpGLR1.2*, *VpGLR1.3*, *VpGLR1.6*, and *VpGLR3.2* were significantly upregulated by at least four-fold on day 10 of infection. This suggested that they contribute to *V. planifolia-F. oxysporum* interaction. These findings provide critical information for the GLR gene family in *V. planifolia* and offer a basis for further functional research.

## Disclosure statement

No potential conflict of interest was reported by the authors.

## Funding

This work was supported by the Guizhou Education Department Youth Science and Technology Talent Growth Project (Qianjiaohe KY Zi [2022] 060) and the Liupanshui Normal University High-level Talents Start-up Fund Project (LPSSYKYJJ201803).

## References

1. Sheng M, Nakagawa T. Glutamate receptors on the move. Nature. 2002;417:601–602. doi:10.1038/417601a.
2. Watkins JC, Jane DE. The glutamate story. Br J Pharmacol. 2006;147:S100–108. doi:10.1038/sj.bjp.0706444.
3. Lam HM, Chiu J, Hsieh MH, Meisel L, Oliveira IC, Shin M, Coruzzi G. Glutamate-receptor genes in plants. Nature. 1998;396:125–126. doi:10.1038/24066.
4. Chiu J, DeSalle R, Lam HM, Meisel L, Coruzzi G. Molecular evolution of glutamate receptors: a primitive signaling mechanism that existed before plants and animals diverged. Mol Biol Evol. 1999;16:826–838. doi:10.1093/oxfordjournals.molbev.a026167.
5. Lacombe B, Becker D, Hedrich R, DeSalle R, Hollmann M, Kwak JM, Schroeder JI, Le Novère N, Nam HG, Spalding EP, et al. The identity of plant glutamate receptors. Science. 2001;292:1486–1487. doi:10.1126/science.292.5521.1486b.
6. Michard E, Lima PT, Borges F, Silva AC, Portes MT, Carvalho JE, Gilliham M, Liu LH, Obermeyer G, Feijó JA. Glutamate receptor-like genes form $Ca^{2+}$ channels in pollen tubes and are regulated by pistil D-serine. Science. 2011;332:434–437. doi:10.1126/science.1201101.
7. Yu B, Sun Y, Jin X, Xie Z, Li X, Huang J. Rice glutamate receptor-like channel OsGLR3.4 modulates the root tropism growth towards amino acids via plasma membrane depolarization and ROS generation. Environ Exp Bot. 2023;205:105146. doi:10.1016/j.envexpbot.2022.105146.
8. Kang J, Turano FJ. The putative glutamate receptor 1.1 (AtGLR1.1) functions as a regulator of carbon and nitrogen metabolism in

*Arabidopsis thaliana*. Proc Natl Acad Sci U S A. 2003;100:6872–6877. doi:10.1073/pnas.1030961100.
9. Chen PY, Hsu CY, Lee CE, Chang IF. *Arabidopsis* glutamate receptor GLR3.7 is involved in abscisic acid response. Plant Signaling & Behavior. 2021;16:1997513. doi:10.1080/15592324.2021.1997513.
10. Zheng Y, Luo L, Wei J, Chen Q, Yang Y, Hu X, Kong X. The glutamate receptors AtGLR1.2 and AtGLR1.3 increase cold tolerance by regulating jasmonate signaling in *Arabidopsis thaliana*. Biochem Biophys Res Commun. 2018;506:895–900. doi:10.1016/j.bbrc.2018.10.153.
11. Lu G, Wang X, Liu J, Yu K, Gao Y, Liu H, Wang C, Wang W, Wang G, Liu M, et al. Application of T-DNA activation tagging to identify glutamate receptor-like genes that enhance drought tolerance in plants. Plant Cell Rep. 2014;33:617–631. doi:10.1007/s00299-014-1586-7.
12. Zhang J, Cui T, Su Y, Zang S, Zhao Z, Zhang C, Zou W, Chen Y, Cao Y, Chen Y, et al. Genome-wide identification, characterization, and expression analysis of glutamate receptor-like gene (GLR) family in sugarcane. Plants (Basel). 2022;11:2440. doi:10.3390/plants11182440.
13. Bjornson M, Pimprikar P, Nürnberger T, Zipfel C. The transcriptional landscape of *Arabidopsis thaliana* pattern-triggered immunity. Nature Plants. 2021;7(5):579–586. doi:10.1038/s41477-021-00874-5.
14. Feng S, Pan C, Ding S, Ma Q, Hu C, Wang P, Shi K. The glutamate receptor plays a role in defense against *Botrytis cinerea* through electrical signaling in tomato. Appl Sci. 2021;11(23):11217. doi:10.3390/app112311217.
15. Yeh CH, Chen KY, Chou CY, Liao HY, Chen HC. New insights on volatile components of *Vanilla planifolia* cultivated in Taiwan. Molecules. 2021;26:3608. doi:10.3390/molecules26123608.
16. Bythrow JD. Vanilla as a medicinal plant. Semin Integr Med. 2005;3:129–131. doi:10.1016/j.sigm.2006.03.001.
17. Gallage NJ, Møller BL. Vanillin-bioconversion and bioengineering of the most popular plant flavor and its de novo biosynthesis in the vanilla orchid. Mol Plant. 2015;8:40–57. doi:10.1016/j.molp.2014.11.008.
18. Buccellato F. Vanilla in perfumery and beverage flavors. In: Havkin-Frenkel D Belanger FC, editors. Handbook of vanilla science and technology. New York: Wiley; 2011. pp. 367–373.
19. Pinaria AG, Liew ECY, Burgess LW. Fusarium species associated with vanilla stem rot in Indonesia. Austral Plant Pathol. 2010;39:176–183. doi:10.1071/AP09079.
20. Solano-De la Cruz MT, Adame-García J, Gregorio-Jorge J, Jiménez-Jacinto V, Vega-Alvarado L, Iglesias-Andreu LG, Escobar-Hernández EE, Luna-Rodríguez M. Functional categorization of de novo transcriptome assembly of *Vanilla planifolia* Jacks. potentially points to a translational regulation during early stages of infection by *Fusarium oxysporum* f. sp. vanillae. BMC Genom. 2019;20:826. doi:10.1186/s12864-019-6229-5.
21. Carbajal-Valenzuela IA, Muñoz-Sanchez AH, Hernández-Hernández J, Barona-Gómez F, Truong C, Cibrián-Jaramillo A. Microbial diversity in cultivated and feral *Vanilla planifolia* orchids affected by stem and rot disease. Microb Ecol. 2022;84:821–833. doi:10.1007/s00248-021-01876-8.
22. Nakamura T, Yamada KD, Tomii K, Katoh K, Hancock J. Parallelization of MAFFT for large-scale multiple sequence alignments. Bioinformatics. 2018;34:2490–2492. doi:10.1093/bioinformatics/bty121.
23. Minh BQ, Schmidt HA, Chernomor O, Schrempf D, Woodhams MD, von Haeseler A, Lanfear R, Teeling E. IQ-TREE 2: new models and efficient methods for phylogenetic inference in the genomic era. Mol Biol Evol. 2020;37:1530–1534. doi:10.1093/molbev/msaa015.
24. Kumar S, Stecher G, Li M, Knyaz C, Tamura K, MEGA X, Battistuzzi FU. Molecular evolutionary genetics analysis across computing platforms. Mol Biol Evol. 2018;35:1547–1549. doi:10.1093/molbev/msy096.
25. Artimo P, Jonnalagedda M, Arnold K, Baratin D, Csardi G, de Castro E, Duvaud S, Flegel V, Fortier A, Gasteiger E, et al. Expasy: sIB bioinformatics resource portal. Nucleic Acids Res. 2012;40(web server issue):W597–603. doi:10.1093/nar/gks400.
26. Huang F, Abbas F, Fiaz S, Imran M, Yanguo K, Hassan W, Ashraf U, He Y, Cai X, Wang Z, et al. Comprehensive characterization of guanosine monophosphate synthetase in *Nicotiana tabacum*. Mol Biol Rep. 2022;49:5265–5272. doi:10.1007/s11033-021-06718-x.
27. Möller S, Croning MD, Apweiler R. Evaluation of methods for the prediction of membrane spanning regions. Bioinformatics. 2001;17:646–653. doi:10.1093/bioinformatics/17.7.646.
28. Chao J, Yingzhen K, Wang Q, Yuhe S, Daping G, Lv J, Guanshan L. MapGene2Chrom, a tool to draw gene physical map based on Perl and SVG languages. Hereditas (Beijing). 2015;37:91–97.
29. Wang Y, Tang H, Debarry JD, Tan X, Li J, Wang X, Lee TH, Jin H, Marler B, Guo H, et al. MCScanX: a toolkit for detection and evolutionary analysis of gene synteny and collinearity. Nucleic Acids Res. 2012;40:e49. doi:10.1093/nar/gkr1293.
30. Bailey TL, Boden M, Buske FA, Frith M, Grant CE, Clementi L, Ren J, Li WW, Noble WS. MEME SUITE: tools for motif discovery and searching. Nucleic Acids Res. 2009;37(web server issue):W202–208. doi:10.1093/nar/gkp335.
31. Hu B, Jin J, Guo AY, Zhang H, Luo J, Gao G. GSDS 2.0: an upgraded gene feature visualization server. Bioinformatics. 2015;31:1296–1297. doi:10.1093/bioinformatics/btu817.
32. Lescot M, Déhais P, Thijs G, Marchal K, Moreau Y, Van de Peer Y, Rouzé P, Rombauts S. PlantCARE, a database of plant *cis*-acting regulatory elements and a portal to tools for in silico analysis of promoter sequences. Nucleic Acids Res. 2002;30:325–327. doi:10.1093/nar/30.1.325.
33. Powell S, Forslund K, Szklarczyk D, Trachana K, Roth A, Huerta-Cepas J, Gabaldón T, Rattei T, Creevey C, Kuhn M, et al. eggNOG v4.0: nested orthology inference across 3686 organisms. Nucleic Acids Res. 2014;42:D231–239. doi:10.1093/nar/gkt1253.
34. Chen C, Chen H, Zhang Y, Thomas HR, Frank MH, He Y, Xia R. Tbtools: an integrative toolkit developed for interactive analyses of big biological data. Mol Plant. 2020;13(8):1194–1202. doi:10.1016/j.molp.2020.06.009.
35. Rao X, Krom N, Tang Y, Widiez T, Havkin-Frenkel D, Belanger FC, Dixon RA, Chen F. A deep transcriptomic analysis of pod development in the vanilla orchid (*Vanilla planifolia*). BMC Genomics. 2014;15(1):964. doi:10.1186/1471-2164-15-964.
36. Grenzi M, Bonza MC, Costa A. Signaling by plant glutamate receptor-like channels: what else! Curr Opin Plant Biol. 2022;68:102253. doi:10.1016/j.pbi.2022.102253.
37. Alfieri A, Doccula FG, Pederzoli R, Grenzi M, Bonza MC, Luoni L, Candeo A, Romano Armada N, Barbiroli A, Valentini G, et al. The structural bases for agonist diversity in an *Arabidopsis thaliana* glutamate receptor-like channel. Proc Natl Acad Sci U S A. 2020;117:752–760. doi:10.1073/pnas.1905142117.
38. Hernández-Coronado M, Dias Araujo PC, Ip PL, Nunes CO, Rahni R, Wudick MM, Lizzio MA, Feijó JA, Birnbaum KD. Plant glutamate receptors mediate a bet-hedging strategy between regeneration and defense. Dev Cell. 2022;57:451–465.e6. doi:10.1016/j.devcel.2022.01.013.
39. Aouini A, Matsukura C, Ezura H, Asamizu E. Characterisation of 13 glutamate receptor-like genes encoded in the tomato genome by structure, phylogeny and expression profiles. Gene. 2012;493:36–43. doi:10.1016/j.gene.2011.11.037.
40. Chiu JC, Brenner ED, DeSalle R, Nitabach MN, Holmes TC, Coruzzi GM. Phylogenetic and expression analysis of the glutamate-receptor-like gene family in *Arabidopsis thaliana*. Mol Biol Evol. 2002;19:1066–1082. doi:10.1093/oxfordjournals.molbev.a004165.
41. Chen J, Jing Y, Zhang X, Li L, Wang P, Zhang S, Zhou H, Wu J. Evolutionary and expression analysis provides evidence for the plant glutamate-like receptors family is involved in woody growth-related function. Sci Rep. 2016;6:32013. doi:10.1038/srep32013.

42. Zhou SH, Zhang L, Lü XZ, Huang JG. Identification and analysis of GLR family genes in maize. J Maize Sci. 2021;2:35–42.
43. Yang L, Zhao Y, Wu X, Zhang Y, Fu Y, Duan Q, Ma W, Huang J. Genome-wide identification and expression analysis of BraGLRs reveal their potential roles in abiotic stress tolerance and sexual reproduction. Cells. 2022;11:3729. doi:10.3390/cells11233729.
44. Teardo E, Carraretto L, De Bortoli S, Costa A, Behera S, Wagner R, Lo Schiavo F, Formentin E, Szabo I. Alter-native splicing-mediated targeting of the *Arabidopsis* glutamate RECEPTOR3.5 to mitochondria affects organelle morphology. Plant Physiol. 2015;167:216–227. doi:10.1104/pp.114.242602.
45. Nguyen CT, Kurenda A, Stolz S, Chételat A, Farmer EE. Identification of cell populations necessary for leaf-to-leaf electrical signaling in a wounded plant. Proc Natl Acad Sci U S A. 2018;115:10178–10183. doi:10.1073/pnas.1807049115.
46. Teardo E, Segalla A, Formentin E, Zanetti M, Marin O, Giacometti GM, Lo Schiavo F, Zoratti M, Szabò I. Characterization of a plant glutamate receptor activity. Cell Physiol Biochem. 2010;26:253–262. doi:10.1159/000320525.
47. Teardo E, Formentin E, Segalla A, Giacometti GM, Marin O, Zanetti M, Lo Schiavo F, Zoratti M, Szabò I. Dual localization of plant glutamate receptor AtGLR3.4 to plastids and plasmamembrane. Biochim Biophys Acta. 2011;1807:359–367. doi:10.1016/j.bbabio.2010.11.008.
48. Lallemand T, Leduc M, Landès C, Rizzon C, Lerat E. An overview of duplicated gene detection methods: why the duplication mechanism has to be accounted for in their choice. Genes. 2020;11–1046. doi:10.3390/genes11091046.
49. Cannon SB, Mitra A, Baumgarten A, Young ND, May G. The roles of segmental and tandem gene duplication in the evolution of large gene families in *Arabidopsis thaliana*. BMC Plant Biol. 2004;4:10. doi:10.1186/1471-2229-4-10.
50. Tanaka KM, Takahasi KR, Takano-Shimizu T. Enhanced fixation and preservation of a newly arisen duplicate gene by masking deleterious loss-of-function mutations. Genet Res (Camb). 2009;91:267–280. doi:10.1017/S0016672309000196.
51. Li F, Wang J, Ma C, Zhao Y, Wang Y, Hasi A, Qi Z. Glutamate receptor-like channel3.3 is involved in mediating glutathione-triggered cytosolic calcium transients, transcriptional changes, and innate immunity responses in *Arabidopsis*. Plant Physiol. 2013;162:1497–1509. doi:10.1104/pp.113.217208.
52. Manzoor H, Kelloniemi J, Chiltz A, Wendehenne D, Pugin A, Poinssot B, Garcia-Brugger A. Involvement of the glutamate receptor AtGLR3.3 in plant defense signaling and resistance to *Hyaloperonospora arabidopsidis*. Plant J. 2013;76:466–480. doi:10.1111/tpj.12311.
53. Kang S, Kim HB, Lee H, Choi JY, Heu S, Oh CJ, Kwon SI, An CS. Overexpression in *Arabidopsis* of a plasma membrane-targeting glutamate receptor from small radish increases glutamate-mediated $Ca^{2+}$ influx and delays fungal infection. Mol Cells. 2006;21:418–427.
54. Liu S, Zhang X, Xiao S, Ma J, Shi W, Qin T, Xi H, Nie X, You C, Xu Z, et al. A single-nucleotide mutation in a glutamate RECEPTOR-LIKE gene confers resistance to fusarium wilt in *Gossypium hirsutum*. Adv Sci (Weinh). 2021;8:2002723.